JGR Atmospheres

RESEARCH ARTICLE
10.1029/2021JD035874

Special Section:
Atmospheric PM2.5 in China: physics, chemistry, measurements, and modeling

Collocated Measurements of Light-Absorbing Organic Carbon in $PM_{2.5}$: Observation Uncertainty and Organic Tracer-Based Source Apportionment

Mingjie Xie[1], Xiang Peng[1], Yue Shang[2], Li Yang[1], Yuanyuan Zhang[1], Yuhang Wang[3], and Hong Liao[1]

[1]Collaborative Innovation Center of Atmospheric Environment and Equipment Technology, Jiangsu Key Laboratory of Atmospheric Environment Monitoring and Pollution Control, School of Environmental Science and Engineering, Nanjing University of Information Science & Technology, Nanjing, China, [2]Shangqiu Bureau of Meteorology, Shangqiu, China, [3]School of Earth and Atmospheric Sciences, Georgia Institute of Technology, Atlanta, GA, USA

Abstract In this study, collocated filter samples of particulate matter with aerodynamic diameter less than 2.5 μm ($PM_{2.5}$) from northern Nanjing were extracted using water and methanol, followed by analysis of light absorption. A backup quartz filter was used to correct sampling artifacts caused by adsorption of gaseous organics. The collocated precision of light-absorbing properties of water-soluble organic carbon (WSOC) and methanol-extractable organic carbon (MEOC) were parameterized using correlation coefficient (r), coefficient of divergence (COD), and average relative percent difference (ARPD, %). In general, the light absorption of WSOC and MEOC showed good agreement ($r > 0.80$, COD < 0.20) between collocated samples. Performing artifact correction is necessary and will increase the heterogeneity between collocated measurements. The duplicate-derived ARPD values of MEOC absorption were more than 60% higher than those of WSOC absorption. Then, it would be inappropriate to assume a uniform uncertainty fraction (e.g., ~10%) for WSOC and MEOC absorption in future studies on their climate effects and source apportionment. To apportion artifact-corrected absorption of aerosol extracts to specific emission sources or formation pathways, positive matrix factorization was performed by using concentration data of selected bulk species and organic molecular markers. Among the nine identified factor/sources, the biomass burning factor had the highest average contributions to the absorption of both WSOC (31.6%) and MEOC (48.0%), followed by dust resuspension and coal combustion factors. Unlike combustion-related primary emissions, the factors containing influences from atmospheric processing (e.g., secondary nitrate) contributed more fractions of WSOC absorption than MEOC absorption.

Key Points:

- Collocated measurements provide an approach to estimate uncertainties in light-absorbing properties of solvent-extractable organic carbon
- Ignoring the adsorption of gaseous organics onto filter medium will lead to significant overestimation of brown carbon absorption
- Aerosol sources influenced by aging processes contributed more fractions of aqueous extracts absorption than methanol extracts absorption

Supporting Information:

Supporting Information may be found in the online version of this article.

Correspondence to:

M. Xie,
mingjie.xie@nuist.edu.cn;
mingjie.xie@colorado.edu

Citation:

Xie, M., Peng, X., Shang, Y., Yang, L., Zhang, Y., Wang, Y., & Liao, H. (2022). Collocated measurements of light-absorbing organic carbon in $PM_{2.5}$: Observation uncertainty and organic tracer-based source apportionment. *Journal of Geophysical Research: Atmospheres*, *127*, e2021JD035874. https://doi.org/10.1029/2021JD035874

Received 15 SEP 2021
Accepted 17 FEB 2022

Author Contributions:

Conceptualization: Mingjie Xie
Funding acquisition: Mingjie Xie
Investigation: Xiang Peng, Yue Shang, Li Yang, Yuanyuan Zhang
Methodology: Mingjie Xie
Project Administration: Mingjie Xie
Supervision: Mingjie Xie
Writing – original draft: Mingjie Xie
Writing – review & editing: Mingjie Xie, Yuhang Wang, Hong Liao

1. Introduction

Organic matter (OM) constitutes a significant fraction (20%–90%) of fine particles with aerodynamic diameter less than 2.5 ($PM_{2.5}$) or 1.0 μm ($PM_{1.0}$; Huang et al., 2014; Jimenez et al., 2009; Sillanpää et al., 2005). Besides potential health impacts, particulate OM can also affect Earth's radiative balance by scattering and absorbing sunlight (Andreae & Gelencsér, 2006; Bond & Bergstrom, 2006; Kirchstetter et al., 2004). Previous ambient or laboratory studies supposed that the particulate OM absorption primarily came from large molecules (e.g., molecular weight, MW > 500–1000 Da) containing conjugated aromatic rings or high degree of unsaturation (Chen & Bond, 2010; Di Lorenzo et al., 2017; Di Lorenzo & Young, 2016; Lin et al., 2014). Due to the spatial heterogeneity in optical properties and sources of light-absorbing organic carbon (termed "brown carbon", BrC), as well as the variability in methods for BrC characterization, their contributions toward the radiative forcing of atmospheric aerosols are not well constrained (Feng et al., 2013; Wang et al., 2014; Yang et al., 2009; Zhang et al., 2017).

In past decades, the light-absorbing properties of BrC, including light absorption coefficients (Abs_λ) and mass absorption efficiency (MAE_λ) at certain wavelengths (λ), absorption Ångström exponent (Å or AAE), and imaginary part (k) of the complex refractive index (RI), were generally retrieved using two types of methods. The first evaluates BrC absorption based on direct particle measurements and Mie theory calculations (Lack et al., 2012; Saleh et al., 2013, 2014). This method characterizes BrC absorption in suspended particles by considering mass concentrations, size distributions, and mixing states of BC and OM, which might be interfered by black carbon (BC) absorption and lensing effect (Pokhrel et al., 2017; Saleh et al., 2015). The other type of method isolated

organic carbon (OC) from BC or elemental carbon (EC) through solvent extraction (e.g., water, methanol) followed by light absorption measurements (Hecobian et al., 2010; Liu et al., 2013; Zhang et al., 2011) and/or molecular characterization (Xie, Chen, et al., 2017; Zhang et al., 2013). Although using the latter method cannot reflect BrC absorption in suspended particles directly, it provides an approach to measure the light absorption of pure OM and identify specific BrC chromophores.

Based on the solvent extraction method, evidences showing that methanol can extract particulate OC more thoroughly (~85%) than water (~50%), and MAE_{λ} values of water-insoluble OC are significantly greater than those of water-soluble fractions (Liu et al., 2013; Xie, Chen, Holder, et al., 2019). However, the uncertainty of aerosol extracts absorption was rarely measured or estimated, which is important for the analysis of BrC radiative forcing and source apportionment. The concentration data of source-specific organic tracers are also prerequisites for source apportionment of BrC (Hecobian et al., 2010; Xie, Chen, Holder, et al., 2019). Polycyclic aromatic hydrocarbons (PAHs) and nitro-aromatic compounds (NACs) are identified as BrC chromophores, and their compositions, mass concentrations, and contributions to BrC absorption have been intensively investigated in ambient and source particles (Huang et al., 2018; Lin et al., 2017; Samburova et al., 2016; Xie, Chen, et al., 2017; Xie et al., 2020). But the identified PAHs and NACs in existing studies are mostly low MW compounds (<300 Da) explaining only a few percentages (<10%) of aerosol extracts absorption, and are not source-specific molecular tracers (Huang et al., 2018; Xie, Chen, Hays, & Holder et al., 2019; Xie et al., 2020). So, measurement data of typical organic tracers (e.g., levoglucosan) are needed for BrC source attribution using receptor models (e.g., positive matrix factorization, PMF).

In this work, collocated $PM_{2.5}$-loaded quartz filter (Q_f) samples were collected in northern Nanjing, China. Each Q_f sample was followed by a backup quartz filter (Q_b) to address positive sampling artifacts. UV/Vis absorbance of methanol-extractable OC (MEOC) and water-soluble OC (WSOC) were measured for all filter samples (Q_f and Q_b). Light-absorbing properties derived from Q_f and $Q_f - Q_b$ data were calculated and compared between collocated samples, so as to generate measurement uncertainties of BrC absorption. Moreover, bulk and molecular speciation data of the same samples were obtained from the companion studies (Gou et al., 2021; Qin et al., 2021; Yang et al., 2021), including water-soluble inorganic ions (WSIIs), bulk OC and EC, WSOC, non-/low-polar and polar organic molecular markers (OMMs), for source apportionment of BrC absorption using PMF model. The present study integrates uncertainty estimation and source apportionment of BrC absorption, and will contribute to future investigations on BrC measurements, sources, and radiative forcing.

2. Methods

2.1. Sampling and Chemical Characterization

Daytime and night-time $PM_{2.5}$ samples were collected at a receptor site located on a seven-story library building in Nanjing University of Information Science and Technology (NUIST, 32.21°N, 118.71°E). Details of the sampling equipment, protocol, and speciation analysis were provided in previous work (Gou et al., 2021; Qin et al., 2021; Yang et al., 2021). Briefly, two identical mid-volume samplers (Sampler I and II; PM2.5-PUF-300, Mingye Environmental, China) installed with 2.5 μm cut-point impactors were set up for collocated sampling at a flow rate of 300 L min^{-1}. Both Sampler I and II were equipped with two pre-baked quartz filters in series (quartz behind quartz, QBQ)—Q_f and Q_b. After the filter pack, gaseous non-/low-polar organic compounds in the air stream were adsorbed using a polyurethane foam (PUF)/XAD-4 resin/PUF (PXP) sandwich in Sampler I, and a PUF plug was installed in Sampler II to capture gaseous polar organics (Figure S1 in the Supporting Information S1). Collocated filter and adsorbent samples were obtained every sixth day from 28 September 2018 to 28 September 2019, and no sample was collected from 16 January 2018 to 21 February 2019 during winter holidays.

All Q_f and Q_b samples from Sampler I and II were used for gravimetric analysis and bulk speciation (WSIIs, OC, EC, and WSOC). WSIIs and WSOC in filter samples were extracted with deionized water (18.2 MΩ). Their concentrations in filtered water extracts were determined using ion chromatography (IC, ICS-3000 and ICS-2000, Dionex, United States) and a total organic carbon analyzer (TOC-L, Shimadzu, Japan), respectively. A thermal-optical carbon analyzer (DRI, 2001A, Atmoslytic, United States) was applied to measure OC and EC following the IMPROVE-A protocol. Chemical analysis and collocated precision of bulk components were provided in Yang et al. (2021). Non-/low-polar OMMs (*n*-alkanes, PAHs, hopanes, and steranes) were quantified for Q_f, Q_b, and PXP samples from Sampler I; polar OMMs (polyol tracers) in Q_f, Q_b, and PUF samples of

Sampler II were analyzed by gas chromatography—mass spectrometer (GC-MS). Measurements and gas-particle partitioning of OMMs were discussed in Gou et al. (2021) and Qin et al. (2021). Table S1 in the Supporting Information S1 summarizes concentration statistics of artifact-corrected bulk components in $PM_{2.5}$ and total OMMs (gas + particle phases).

2.2. Light Absorption Measurement

Collocated Q_f and Q_b samples were extracted using water and methanol, followed by light absorbance measurement with a UV/Vis spectrometer (UV-1900, Shimadzu Corporation) over the wavelength (λ) range of 200–900 nm. The procedures for light absorption measurement of aerosol extracts were generally the same as those in Xie, Hays, & Holder (2017), Xie, Chen, Holder, et al. (2019). One fourth of each quartz filter (~50 cm^2) was sonicated in 40 mL pure water (18.2 MΩ) for 30 min. The light absorbance of aqueous extracts ($A_{\lambda,w}$) was determined after passing through a 25 mm diameter polytetrafluorethylene (PTFE) filter (0.22 μm pore size, Anpel Laboratory Technologies, China), and was converted to light absorption coefficient ($Abs_{\lambda,w}$, Mm^{-1}) by

$$Abs_{\lambda,w} = (A_{\lambda,w} - A_{700,w}) \times \frac{V_l}{V_a \times L} \ln(10) \quad (1)$$

where $A_{700,w}$ is used to adjust systematic baseline drift, V_l (m^3) denotes solvent extract volume, V_a (m^3) represents sampled air volume of the extracted filter area, L (0.01 m) is the optical path length of the quartz cuvette in UV/Vis spectrometer, and ln (10) changes $Abs_{\lambda,w}$ from common to natural logarithm (Hecobian et al., 2010). The solution mass absorption efficiency ($MAE_{\lambda,w}$, $m^2\ g^{-1}$ C) is used to normalize $Abs_{\lambda,w}$ of each sample by its WSOC concentration (μg m^{-3})

$$MAE_{\lambda,w} = \frac{Abs_{\lambda,w}}{WSOC} \quad (2)$$

and the extraction efficiency of water (η_w, %) is expressed as

$$\eta_w = \frac{WSOC}{OC} \times 100\% \quad (3)$$

The solution absorption Ångström exponent ($Å_w$), depicting wavelength dependence of the aqueous extract absorption, was set as the absolute value of the regression slope of lg ($Abs_{\lambda,w}$) versus lg(λ) over 300–550 nm.

To evaluate the light-absorbing properties of MEOC, another aliquot (~6 cm^2) of each filter sample was extracted ultrasonically in 10 mL of methanol, followed by filtration and light absorbance measurement in a same manner as water extracts. After extraction, filter samples were air dried in a fume hood and analyzed for residual OC (rOC, μg m^{-3}) using the thermal-optical carbon analyzer. Concentrations of MEOC was obtained by subtracting rOC from OC in samples before extraction (Chen & Bond, 2010; Xie et al., 2018), Xie, Chen, Holder, et al. (2019). The extraction efficiency of methanol (η_m, %) is calculated by

$$\eta_m = \frac{MEOC}{OC} \times 100\% \quad (4)$$

The η_m values of Q_b samples were assumed to be 100% as their average rOC (0.050 μg m^{-3}) was comparable to the method detection limit (MDL, 0.066 μg m^{-3}). Similar to Equations 1 and 2, the light absorption coefficient of methanol extract ($Abs_{\lambda,m}$) is defined as

$$Abs_{\lambda,m} = (A_{\lambda,m} - A_{700,m}) \times \frac{V_l}{V_a \times L} \ln(10) \quad (5)$$

and is normalized by MEOC to derive mass absorption efficiency ($MAE_{\lambda,m}$, $m^2\ g^{-1}$ C)

$$MAE_{\lambda,m} = \frac{Abs_{\lambda,m}}{MEOC} \quad (6)$$

Since the loss of methanol insoluble OC from filter samples during sonication was neglected, values of MEOC and η_m were presented as upper limits, and $MAE_{\lambda,m}$ values were given as lower limits. The absorption Ångström exponent of methanol extract ($Å_m$) is determined identically as $Å_w$. To compare with previous studies, Abs_λ and

MAE_{λ} values at 365 nm were presented and discussed in this work. However, most ambient studies evaluated BrC absorption by sampling PM using a single quartz filter, ignoring the adsorption of gaseous organics onto filter medium. Here, Q_b measurements were used to correct BrC absorption in $PM_{2.5}$ as follows

$$\text{Artifact}-\text{corrected}\ \ \text{Abs}_{\lambda,w/m} = \text{Abs}^{Qf}_{\lambda,w/m} - \text{Abs}^{Qb}_{\lambda,w/m} \tag{7}$$

$$\text{Artifact}-\text{corrected}\ \ \text{MAE}_{\lambda,w} = \frac{\text{Abs}^{Qf}_{\lambda,w} - \text{Abs}^{Qb}_{\lambda,w}}{\text{WSOC}_{Qf} - \text{WSOC}_{Qb}} \tag{8}$$

$$\text{Artifact}-\text{corrected}\ \ \text{MAE}_{\lambda,m} = \frac{\text{Abs}^{Qf}_{\lambda,m} - \text{Abs}^{Qb}_{\lambda,m}}{\text{MEOC}_{Qf} - \text{OC}_{Qb}} \tag{9}$$

where $\text{Abs}^{Qf}_{\lambda,m/w}$ and $\text{Abs}^{Qb}_{\lambda,m/w}$ are light absorption coefficients of Q_f and Q_b samples, respectively, in water or methanol extracts; WSOC_{Qf} and WSOC_{Qb} are WSOC concentrations in Q_f and Q_b samples; and MEOC_{Qf} and OC_{Qb} are MEOC and OC concentrations in Q_f and Q_b samples. Artifact corrected $\mathring{A}_{w/m}$ were derived from the regression slope of lg ($\text{Abs}^{Qf}_{\lambda,m/w}$− $\text{Abs}^{Qb}_{\lambda,m/w}$) versus lg($\lambda$) over 300–550 nm. Then the corrected extraction efficiencies of water and methanol are calculated as

$$\text{Artifact}-\text{corrected}\ \ \eta_w = \frac{\text{WSOC}_{Qf} - \text{WSOC}_{Qb}}{\text{OC}_{Qf} - \text{OC}_{Qb}} \times 100\% \tag{10}$$

$$\text{Artifact}-\text{corrected}\ \ \eta_m = \frac{\text{MEOC}_{Qf} - \text{OC}_{Qb}}{\text{OC}_{Qf} - \text{OC}_{Qb}} \times 100\% \tag{11}$$

2.3. Collocated Precision Analysis

Pearson's correlation coefficient (r) and coefficients of divergence (COD) were calculated to examine the similarity in light-absorbing properties of water and methanol extracts between collocated measurements, and the COD is defined as (Wilson et al., 2005)

$$\text{COD}_{12} = \sqrt{\frac{1}{n}\sum_{i=1}^{n}\left(\frac{x_{i1} - x_{i2}}{x_{i1} + x_{i2}}\right)^2} \tag{12}$$

where x_{i1} and x_{i2} are the same light-absorbing property for ith sample from Sampler I and II, and n denotes the size of paired samples. The correlation coefficient is a statistical measure of how collocated measurements vary together (Kim et al., 2005), but cannot be used to evaluate the similarity in magnitude. The COD informs the degree of uniformity between two variables. In this work, COD values close to 1 and 0 suggest non- and full consistency between collocated BrC measurements (Kim et al., 2005; Wilson et al., 2005; Wongphatarakul et al., 1998). A boundary COD value of 0.2 was typically used to indicate significant difference between pairs of measurements (Krudysz et al., 2008; Xie et al., 2012). The average relative percent difference (ARPD, %) can be used to estimate measurement uncertainty derived from duplicate data (Dutton et al., 2009; Flanagan et al., 2006), and is defined as

$$\text{ARPD} = \frac{2}{n}\sum_{i=1}^{n}\frac{|x_{i1} - x_{i2}|}{(x_{i1} + x_{i2})} \times 100\% \tag{13}$$

2.4. PMF Source Apportionment

To attribute the light-absorption of aerosol extracts to specific sources, PMF version 5.0 (U.S. Environmental Protection Agency) was applied by involving concentration data of $PM_{2.5}$ bulk components and several groups of OMMs. The speciation data of bulk components and OMMs were obtained from our previous work (Gou et al., 2021; Qin et al., 2021; Yang et al., 2021) and prepared as detailed in the Supplement (Text S1 in the Supporting Information S1). The final input data set contained 102 observations of 11 artifact-corrected bulk

Table 1
Concentrations of Extractable Organic Components and Their Light-Absorbing Properties in Collocated Q_f and Q_b Samples

	Sampler I				Sampler II			
	No. of obs.	Median	Mean ± std	Range	No. of obs.	Median	Mean ± std	Range
Q_f								
OC, μg m^{-3},[a]	103	8.32	8.80 ± 3.70	2.29–18.7	109	7.51	8.41 ± 3.69	2.44–20.1
WSOC, μg m^{-3},[a]	103	4.83	5.16 ± 2.33	1.57–12.4	109	4.56	4.99 ± 2.35	1.45–12.2
MEOC, μg m^{-3}	103	6.94	7.15 ± 2.93	2.06–15.3	109	6.25	6.85 ± 2.87	1.84–15.8
η_w,%	103	59.6	59.2 ± 9.94	30.0–85.0	109	60.5	59.6 ± 9.90	28.3–86.4
η_m,%	103	83.0	81.7 ± 9.35	52.2–99.6	108	84.1	82.9 ± 9.59	54.9–98.2
$Abs_{365,w}$, Mm^{-1}	103	2.70	3.30 ± 1.91	0.43–8.65	109	2.64	3.24 ± 2.18	0.47–13.7
$MAE_{365,w}$, m^2 g^{-1} C	103	0.59	0.64 ± 0.28	0.10–1.47	109	0.58	0.64 ± 0.29	0.18–1.47
$Å_w$	103	7.16	7.12 ± 1.04	4.31–11.1	109	7.21	7.10 ± 1.12	4.17–9.54
$Abs_{365,m}$, Mm^{-1}	103	7.04	7.78 ± 4.27	0.95–19.2	109	6.57	7.78 ± 5.01	0.95–31.3
$MAE_{365,m}$, m^2 g^{-1} C	103	1.01	1.15 ± 0.57	0.28–2.59	109	0.99	1.16 ± 0.58	0.26–3.08
$Å_m$	103	5.87	6.13 ± 1.41	4.34–11.9	109	5.73	6.16 ± 1.45	4.26–10.6
Q_b								
OC, μg m^{-3},[a]	102	0.61	0.76 ± 0.52	0.061–2.29	108	0.64	0.80 ± 0.59	0.067–3.32
WSOC, μg m^{-3},[a]	103	0.57	0.64 ± 0.35	0.054–1.90	109	0.58	0.64 ± 0.35	0.037–2.22
$Abs_{365,w}$, Mm^{-1}	85	0.43	0.43 ± 0.29	0.085–1.11	92	0.28	0.38 ± 0.37	0.085–1.96
$Abs_{365,m}$, Mm^{-1}	98	0.88	0.98 ± 0.74	0.16–4.47	104	0.87	0.99 ± 0.71	0.16–4.09

[a]Obtained from Yang et al. (2021).

species ($Abs_{365,w}$, $Abs_{365,m}$, 5 WSIIs, OC, EC, WSOC, MEOC) and 50 OMMs (gas + particle phases). Uncertainties of bulk components concentrations and aerosol extracts absorption were set as their ARPD values, and those of OMMs were estimated in a same manner as Xie et al. (2016), Xie, Chen, Holder, et al. (2019). Missing values and measurements below detection limits (BDL) were substituted by the geometric mean of all observations and half of the detection limit, respectively. Their accompanying uncertainties were set to four times the geometric mean and five-sixths the detection limit (Polissar et al., 1998). The PMF model is a multivariate statistical technique and resolves factor/source profiles and contributions from a concentration data matrix of source markers. In this work, the input data set was tested for four-to ten-factor PMF solutions, and the final factor number was determined primarily based on the interpretability of each base-case solution (Text S1 in the Supporting Information S1).

3. Results and Discussion

3.1. Measurement Results Summary

Concentrations and light-absorbing properties of WSOC and MEOC in Q_f and Q_b samples from Sampler I and II are summarized in Table 1. Measurement results of OC and WSOC concentrations were obtained from Yang et al. (2021) and used for the calculation of extraction efficiency and MAE_λ. As the carbon content on Q_b was attributed to the adsorption of volatile or semi-volatile organics in gas phase ("positive artifact"), only light absorption coefficients ($Abs_{365,w}$ and $Abs_{365,m}$) of Q_b extracts were provided for artifact corrections. Generally, no significant difference ($p > 0.25$) in averages of all measurements between Sampler I and II was observed (Table 1). Figures 1 and 2 show comparisons between collocated measurements of MEOC concentrations, extraction efficiencies of water (η_w) and methanol (η_m), and light-absorbing properties of WSOC ($Abs_{365,w}$, $MAE_{365,w}$, and $Å_w$) and MEOC ($Abs_{365,m}$, $MAE_{365,m}$, and $Å_m$) prior to and after Q_b corrections. Pearson's correlation coefficient (r), COD, and ARPD values are also included in Figures 1 and 2. Collocated comparison results of OC, WSOC, and other PM bulk components (e.g., WSIIs) have been reported and discussed in Yang et al. (2021).

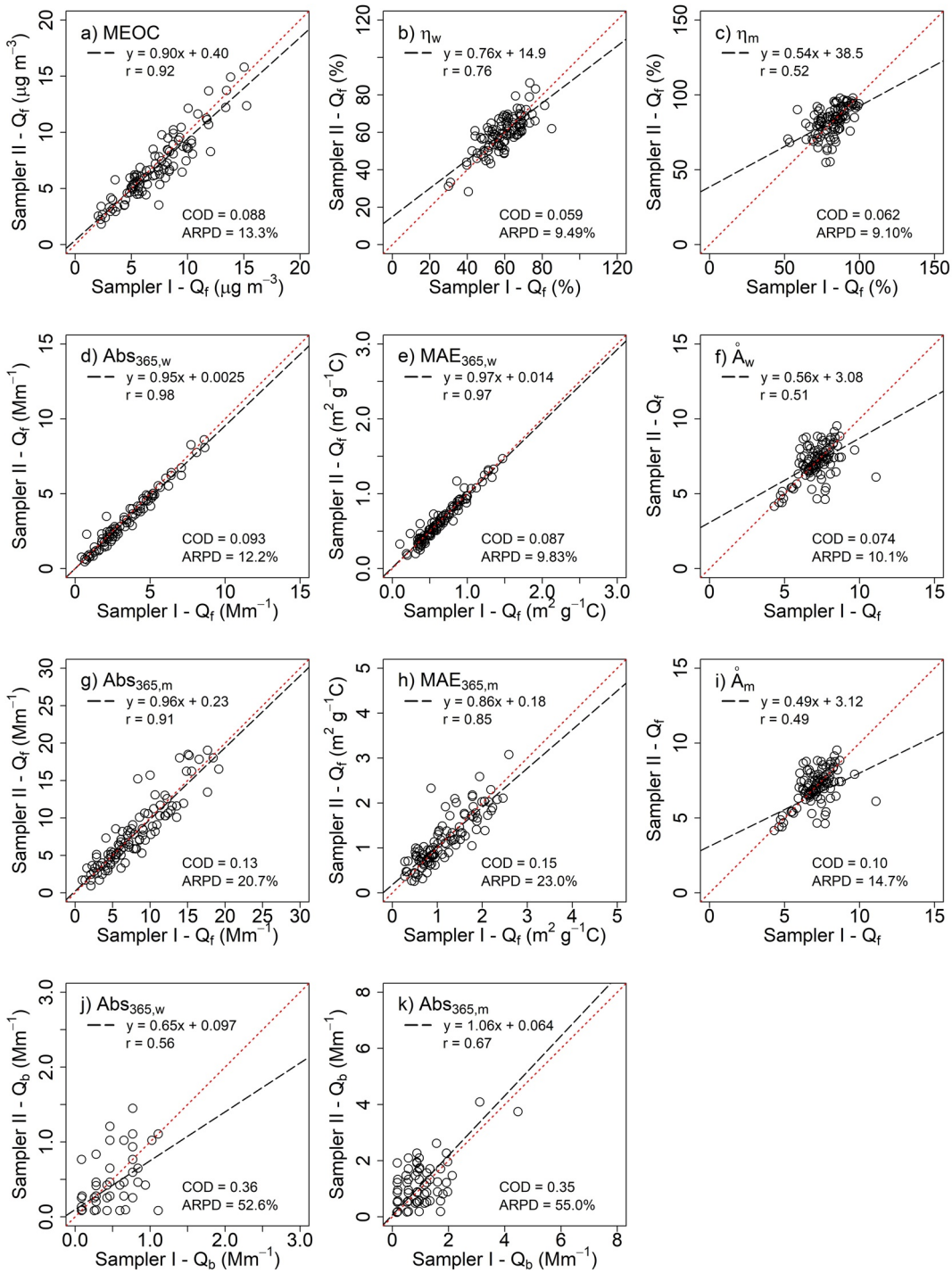

Figure 1. Comparisons between collocated Q_f and Q_b analysis for light-absorbing properties of aerosol extracts.

3.2. Comparisons of Collocated Q_f Measurements

In Figure 1, all comparisons between collocated Q_f samples exhibit low divergence with COD <0.20 (0.059 – 0.15), although η_w, $Å_w$, and $Å_m$ have moderate correlations ($r = 0.49 – 0.52$). The comparison of MEOC concentrations between collocated Q_f samples ($r = 0.92$, COD = 0.088) showed greater divergence than OC ($r = 0.98$, COD = 0.062) and WSOC ($r = 0.99$, COD = 0.041; Yang et al., 2021). OC and WSOC were measured directly from filter samples and filter extracts, respectively, whereas MEOC was calculated by subtracting residual OC

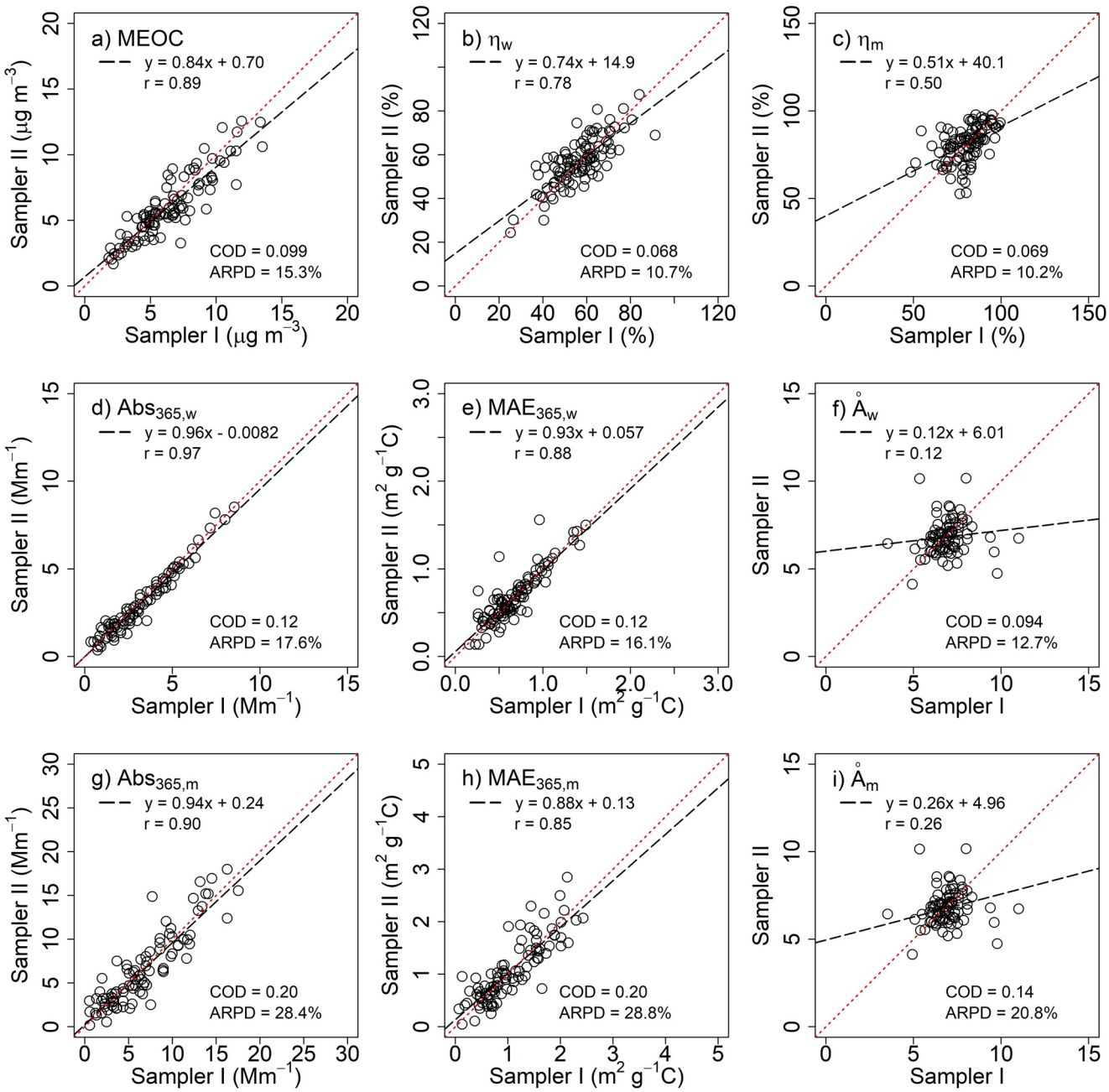

Figure 2. Comparisons between collocated measurements for light-absorbing properties of aerosol extracts after Q_b corrections.

from OC in the filter prior to methanol extraction. So, the collocated precision of MEOC was impacted by uncertainties of multiple measurements. Moreover, some insoluble organic particles might come off the filter during the extraction process, leading to overestimated MEOC concentrations and η_m. Li et al. (2016) determined MEOC from pyrolysis of corn stalk by pipetting a certain volume (30 μL) of sample extracts onto a blank filter punch and analyzing its OC content when the extract was dried. This method can eliminate the influence of detached insoluble organics on MEOC, but requires extremely high OC loadings (e.g., source emission samples) and might not be applicable to ambient samples. Although η_w and η_m had comparable fractional uncertainties (ARPD = 9.49% and 9.10%) and COD (0.059 and 0.062), the scatter data of η_m mostly clustered on the 1:1 line and showed less variability than η_w (Table 1 and Figures 1b and 1c). This can be ascribed to the fact that methanol has stronger dissolving capability than water, and η_m was overestimated due to the loss of some insoluble OC.

Comparisons of $Abs_{365,w}$ ($r = 0.98$, COD = 0.093, and ARPD = 12.2%) and $MAE_{365,w}$ ($r = 0.97$, COD = 0.087, and ARPD = 9.83%) showed better agreement than those for $Abs_{365,m}$ ($r = 0.91$, COD = 0.13, ARPD = 20.7%) and $MAE_{365,m}$ ($r = 0.85$, COD = 0.15, ARPD = 23.0%, Figure 1). Here, 1/4 (50 cm^2) and 6 cm^2 of Q_f samples were extracted using water and methanol, respectively. It was suggested that the collocated precision was better for analysis performed on a large portion of filter in comparison to small aliquots (Hyslop & White, 2008). Similar to η_m, the scatter data of $Å_w$ and $Å_m$ mostly clustered with little variability (Table 1 and Figures 1f and 1i). Although the absorption Ångström exponents of suspended particles (AAE) vary across primary emission sources (Kirchstetter et al., 2004), cautions are warranted when implementing source apportionment of light-absorbing carbonaceous aerosols based on AAE values, as the spectral dependence of light absorption also depends on fuel types and burn conditions of specific combustion sources (Helin et al., 2021). In this work, $Å_w$ and $Å_m$ reflected the spectral dependence of WSOC and MEOC absorption, which were not influenced by other light-absorbing materials (e.g., BC, dust) in ambient aerosols. However, no source information could be retrieved, as the spectral dependence of BrC absorption from a variety of primary combustion sources had similar characteristics depending largely on fuel types and burn conditions (Chen & Bond, 2010; Xie, Chen, Hays, & Holder et al., 2019; Xie, Hays, & Holder, 2017; Xie et al., 2018).

3.3. Artifact Corrections and Uncertainty Estimations

The bulk carbon detected on Q_b was often subtracted from Q_f measurements to address the positive sampling artifact (Chow et al., 2010; Subramanian et al., 2004; Yang et al., 2021). While very few field studies measured the light absorption of OC and WSOC in Q_b samples, which could be considered as positive sampling artifacts of BrC. Xie et al. (2018) applied the QBQ method to investigate the light absorption of OC from a variety of fuel-cookstove combinations, and the $MAE_{365,m}$ value did not change significantly ($p > 0.05$) after Q_b correction, indicating that the light absorption of OC in source particles are dominated by low-volatile organics. Similar to WSOC, average $Abs_{365,w}$ and $Abs_{365,m}$ of Q_b samples were 11%–13% of Q_f measurements (Table 1). The large heterogeneity of $Abs_{365,w}$ and $Abs_{365,m}$ between collocated Q_b samples was reflected by their moderate correlations ($r < 0.70$), high COD (>0.30) and ARPD (>50%) values (Figures 1j and 1k). Possible explanations are as follows: Q_b has much lower OC concentrations than Q_f (Table 1). A certain fraction of OC adsorbed on filter medium might be lost during sampling and filter handling (transportation, storage, and conditioning prior to gravimetric analysis). Quartz filters with similar surface area might not have exactly the same adsorption capacity for gaseous organics (Kirchstetter et al., 2001).

After Q_b corrections, concentrations of bulk carbon and their solvent extracts absorption during daytime, nighttime, and the whole day are summarized in Table S2 in the Supporting Information S1. The averages of WSOC and MEOC concentrations, $Abs_{365,w}$, $Abs_{365,m}$, and $MAE_{365,m}$ in Q_f samples were more than 10% ($p < 0.01$) greater than those after Q_b corrections. Then if positive sampling artifacts of OC were ignored, the light absorption of solvent extracts will be significantly overestimated. Because the difference in Q_b corrections between collocated observations was accounted for, the duplicate-derived correlations ($r = 0.12 – 0.97$), COD values (0.094 – 0.20), and uncertainty estimates (ARPD = 12.7% – 28.8%) of light-absorbing properties using artifact-corrected data suggested a level of agreement lower than that for collocated Q_f measurements ($r = 0.49 – 0.98$, COD = 0.074 – 0.13, and ARPD = 9.83%–23.0%; Figures 1 and 2). As mentioned in the introduction, reliable uncertainty estimates are needed for the analysis of BrC radiative forcing and source apportionment. However, there is a relative dearth of uncertainty estimation for solvent extracts absorption of aerosol samples, and collocated measurements are an appropriate method evaluating the total uncertainty of sampling and laboratory analysis. Based on collocated observations, Yang et al. (2021) found that assuming an uncertainty fraction of 10% was reasonable for $PM_{2.5}$ major components (e.g., NH_4^+, SO_4^{2-}, and OC). But it will underestimate the uncertainties of low-concentrated species (e.g., Ca^{2+} and Mg^{2+}) and light-absorbing properties of solvent extracts in this work. Because uncertainty data are mandatory for receptor modeling to reduce the impacts of noise on observation data, the source apportionment results will be subject to large errors if proper estimates of uncertainties were not obtained (Kim & Hopke, 2007; Paatero & Hopke, 2003). The ARPD values of $PM_{2.5}$ components and light-absorbing properties of WSOC and MEOC provided by Yang et al. (2021) and this work can be used as their uncertainty fractions in future studies.

3.4. Temporal Variations and Magnitudes

Time series of bulk carbon concentrations and their light-absorbing properties of Q_f and Q_b samples are shown in Figures S2 and S3 in the Supporting Information S1. Temporal patterns of WSOC, MEOC, and their absorption were almost identical between collocated Q_f samples (Figure S2 in the Supporting Information S1), while $Abs_{365,w}$ and $Abs_{365,m}$ of collocated Q_b samples exhibited less consistency probably due to high uncertainties (Figures 1j and 1k, and S3 in the Supporting Information S1). Unlike bulk OC and WSOC concentrations, of which the temporal variations were not obvious, Abs_{365} and MAE_{365} values of both water and methanol extracts of Q_f samples exhibited maxima in winter and minima in summer (Figure S2 in the Supporting Information S1), and performing Q_b corrections did not change their seasonal patterns (Figure S4 in the Supporting Information S1). One possible explanation is that BrC from primary emission sources (e.g., biomass/biofuel burning, fossil fuel combustions) has stronger light absorption than that generated through photochemical reactions (Wang, et al., 2019), and can undergo more photobleaching in summer than in winter. $Abs_{365,m}$ and $MAE_{365,m}$ of Q_f samples showed more significant day-night difference ($p = 0.06 – 0.08$, Figure S2 in the Supporting Information S1) than $Abs_{365,w}$ ($p = 0.27$) and $MAE_{365,w}$ ($p = 0.28$). Similar comparison results were also obtained using artifact-corrected data (Figure S4 in the Supporting Information S1), indicating that the water-insoluble BrC chromophores might be more vulnerable to sunlight. Although $Å_w$ and $Å_m$ had little variability, negative linear relationships were observed for $Å_w$ versus $MAE_{365,w}$ and $Å_m$ versus $MAE_{365,m}$ (Figure S5 in the Supporting Information S1). Moreover, $Å_m$ values were significant smaller ($p < 0.05$) than $Å_w$, while $MAE_{365,m}$ values were more than 50% larger than $MAE_{365,w}$ (Tables 1 and S2 in the Supporting Information S1). These results reflect the fact that the absorption of strong BrC chromophores depends less on wavelength than weak BrC (Xie, Hays, & Holder, 2017; Xie, Chen, Holder, et al., 2019).

Since positive artifact corrections using Q_b measurements were rarely performed in ambient studies on BrC absorption, measurement results of collocated Q_f samples were averaged to compare with other field work in Table S3 in the Supporting Information S1. From 2015 to 2019, concentrations of bulk carbon (OC, WSOC, and MEOC) and their light absorption in solvent extracts exhibited a decreasing trend in eastern Chinese cities, particularly for the NUIST site, which could be attributed to the implementation of the Air Pollution Prevention and Control Action Plan (2013–2017) and Three-year Action Plan to Fight Air Pollution (2018–2020) by the State Council of China. Bulk carbon concentrations and Abs_{365} values varied greatly across Chinese and US cities due to the spatial-temporal heterogeneity of their sources (Table S3 in the Supporting Information S1). MAE_{365} values of Chinese cities ($MAE_{365,w} = 0.64 – 1.24\ m^2\ g^{-1}C$, $MAE_{365,m} = 0.93 – 1.54\ m^2\ g^{-1}C$) were comparable to those observed in Los Angeles ($MAE_{365,w} = 0.71\ m^2\ g^{-1}C$, $MAE_{365,w} = 1.56\ m^2\ g^{-1}C$; Zhang et al., 2011, 2013), but more than two times larger than observations in Southeastern US (Table S3 in the Supporting Information S1), where the BrC was less contributed by biomass burning and anthropogenic fossil carbon (Xie, Chen, Holder, et al., 2019; Zhang et al., 2011). The average η_w and η_m values showed smaller difference between Chinese and US cities (η_w 50%–60%, η_m 80%–90%) than Abs_{365}. Considering that the η_m of freshly emitted OC from combustion sources has a narrow range (75–95%; Chen & Bond, 2010; Xie, Hays, & Holder, et al., 2017, Xie et al., 2018), the similarity in η_m across source emissions and ambient PM might be partly attributed to the ignorance of the detachment of insoluble OC during extraction. The undissolved fraction of OC in methanol is likely composed of large and highly conjugated molecules, and their physicochemical properties (e.g., structure, light absorption) are unknown and warrant further study.

3.5. PMF Source Apportionment

A nine-factor solution was finally determined based on the interpretability of resolved factors. Although four-to six-factor solutions are more robust with higher factor matching rates of bootstrapping (BS) runs and less factor swaps during BS-displacement (DISP) analysis (Table S4 in the Supporting Information S1), the input species are related with more than six specific emission sources and formation pathways. Moreover, median and mean levels of artifact-corrected $Abs_{365,w}$, $Abs_{365,m}$, and bulk components had good agreement between PMF estimations and observed data (Table S5 in the Supporting Information S1), indicating that the nine-factor solution can reasonably reproduce the averages and temporal variations of input species. Figure 3 presents factor profiles normalized as

$$F_{kj}^{*} = \frac{F_{kj}}{\sum_{k=1}^{p} F_{kj}} \tag{14}$$

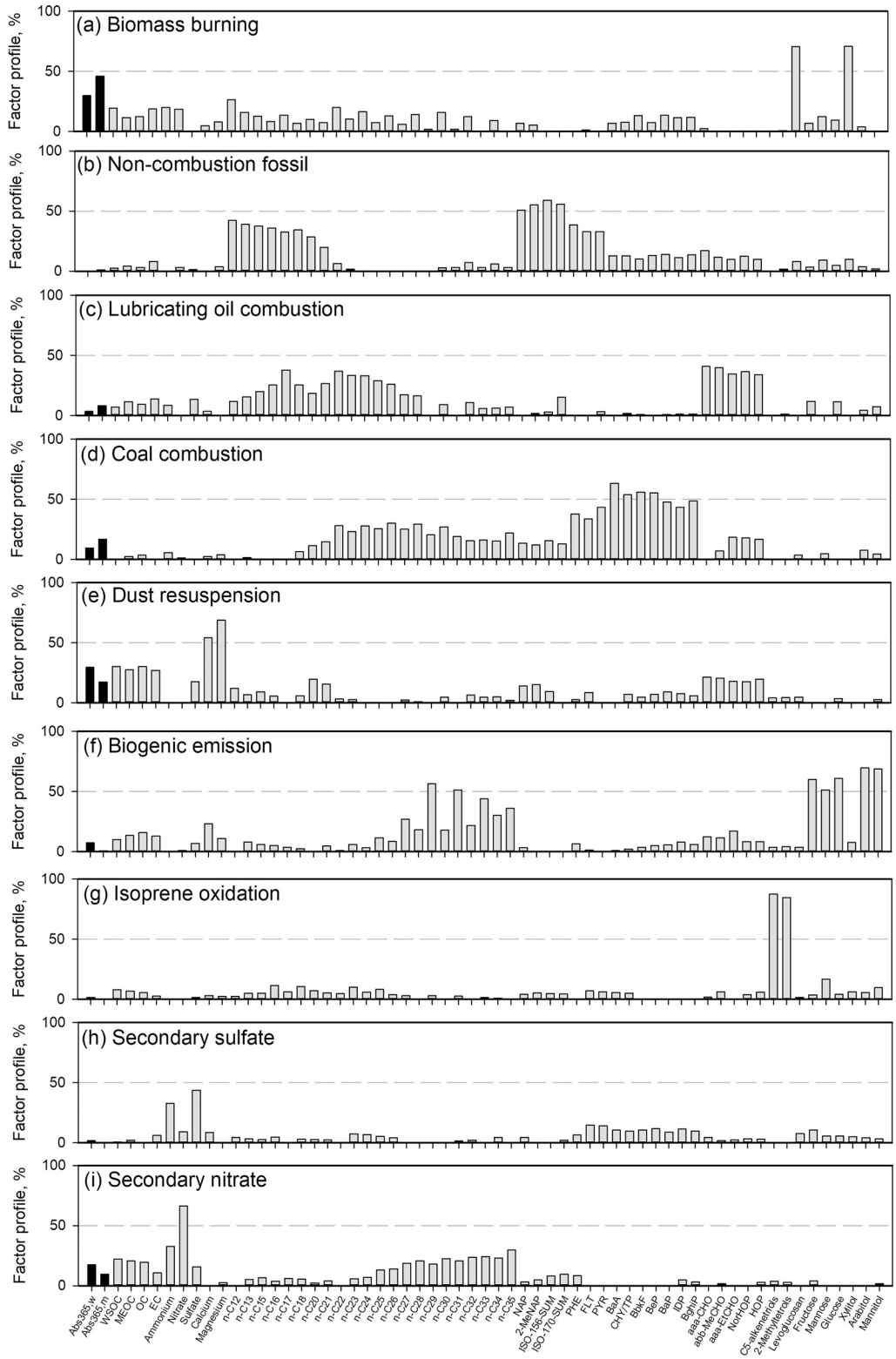

Figure 3. Normalized factor profiles of the 9-factor PMF solution. Black bars represent $Abs_{365,w}$ and $Abs_{365,m}$.

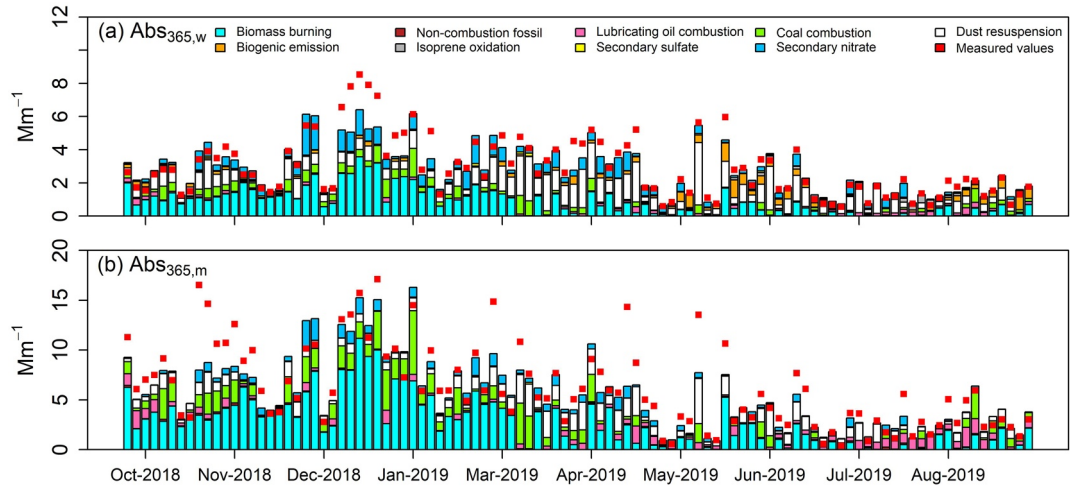

Figure 4. Factor contribution distributions of (a) $Abs_{365,w}$ and (b) $Abs_{365,m}$ in each day of the whole sampling period.

where F^*_{kj} (%) is the weighted abundance of species j in factor k. The factor contribution distributions of solvent extracts absorption and $PM_{2.5}$ major components are shown in Figures 4 and S6 in the Supporting Information S1, respectively. Here, the resulting nine factors were linked with biomass burning, non-combustion fossil, lubricating oil combustion, coal combustion, dust resuspension, biogenic emission, isoprene oxidation, secondary sulfate, and secondary nitrate individually. Their average relative contributions to $Abs_{365,w}$, $Abs_{365,m}$, and bulk carbon components are listed in Table S6 in the Supporting Information S1. The eight-factor solution cannot separate secondary sulfate and nitrate factors; the ten-factor solution resolves an unexplainable factor, of which the characteristic species (steranes, hopanes, and sugar alcohols) are indicators of different sources.

In Figure 3a, the biomass burning factor was resolved based on the highest loading of levoglucosan, a tracer of cellulose pyrolysis (Simoneit et al., 1999). This factor had the largest average relative contributions to $Abs_{365,w}$ (31.6%) and $Abs_{365,m}$ (48.0%), and dominated solvent extracts absorption mainly in cold periods (Figure 4). Considering that the study location is ~5 km to the border of Jiangsu and Anhui provinces and close to rural communities (<2 km), and levoglucosan is subject to significant atmospheric degradation (lifetime 1.8 days; Li et al., 2021), biomass and biofuel combustions from surrounding rural areas are expected to be important BrC sources in winter. Soil and associated microbiota (e.g., bacteria, fungi) are a typical source of saccharide polyols in ambient aerosols (Simoneit et al., 2004), whereas xylitol in the atmosphere of northern Nanjing was primarily contributed by biomass burning (Figure 3a).

The non-combustion fossil, lubricating oil combustion, and coal combustion factors were identified and well defined in a companion study (Gou et al., 2021), where the influence of gas/particle portioning of non-/low-polar OMMs on source apportionment was examined. The non-combustion fossil factor contains large fractions of low MW *n*-alkanes and PAHs (Figure 3b). Since these compounds are enriched in unburned diesel fuel and motor oil (Schauer et al., 1999), and large-scale petrochemical industries are ~6 km to the northeast of the sampling site, this factor should be related to evaporation emissions from crude oil and petroleum products. The lubricating oil combustion factor consisted mainly of sterane and hopanes and had a *n*-alkane profile resembling engine lubricating oil (Carvaggio et al., 2007). Chen et al. (2001) found that the EC emission from motor vehicles increased when the ambient temperature exceeded a threshold of 17°C, and attributed the elevated emissions from motor vehicles on hot days to low intake air density (Human et al., 1990). This might also be one possible explanation for increased contributions from the lubricating oil combustion factor in summer. In southern Chinese cities, the meteorological conditions (e.g., low boundary layer height) and transport of coal burning emissions from northern cities are responsible for elevated particulate PAHs concentrations in winter (Liu, Lin, et al., 2017; Liu, yan, et al., 2017; Wang, et al., 2019; Yan et al., 2019). So, the factor characterized by medium to high MW PAHs were linked with coal combustion. This factor had the second highest average contribution to $Abs_{365,m}$ (18.5%, Table S6 in the Supporting Information S1), supporting that PAHs could act as one category of water-insoluble BrC chromophores (Huang et al., 2020; Zhu et al., 2020). These three fossil fuel-related primary sources were also identified in urban Denver, USA (Xie, Barsanti, et al., 2013; Xie, Piedrahita et al., 2013; Xie et al., 2014), and

had more contributions to $Abs_{365,m}$ than $Abs_{365,w}$ (Table S6 in the Supporting Information S1). This is because fossil fuel-related primary organics are characterized by hydrophobic compounds (e.g., *n*-alkanes, PAHs; Rogge et al., 1993a; Schauer et al., 1999, 2002), and their contributions to MEOC (2.95%–11.0%) were also higher than WSOC (0%–7.00%, Table S6 in the Supporting Information S1).

The dust resuspension factor accounted for most Ca^{2+} and Mg^{2+} fractions, and contributed 26.9% and 15.7% of $Abs_{365,w}$ and $Abs_{365,m}$. Due to the presence of bulk carbon components (e.g., EC), steranes and hopanes, the dust resuspension factor might be primarily influenced by on-road traffic emissions. Yu et al. (2020) performed PMF analysis for $PM_{2.5}$ using elements data from an urban site in Nanjing, and more than 50% of OC and EC were lumped in an on-road traffic factor due to the lack of OMMs. In this work, the dust resuspension factor also had the highest average contributions to OC (27.1%) and EC (24.6%), especially in spring with the lowest relative humidity of the year (Yu et al., 2019). Unlike primary combustion related factors, the organic components in dusts experience more heterogeneous aging process and become hygroscopic (Maria et al., 2004), leading to comparable absolute contributions to $Abs_{365,w}$ ($0.87 \pm 0.70\ Mm^{-1}$) and $Abs_{365,m}$ ($1.05 \pm 0.84\ Mm^{-1}$).

The biogenic emission factor contained the highest percentages of saccharide polyols, and had a *n*-alkane pattern with clear odd-to-even carbon number predominance. These characteristics indicated microbiota activities and decomposition of plant materials in soil (Rogge et al., 1993c; Simoneit et al., 2004). Then the small fractions of bulk carbon components and Ca^{2+}, Mg^{2+} loaded on this factor could be ascribed to surface soil resuspension. The isoprene oxidation factor dominated the profiles of C5-alkene triols and 2-methyltetrols—tracers for isoprene SOA products (Claeys et al., 2004; Surratt et al., 2006). Given the dominance of biogenic origins, the elevated contributions of these two factors to organic substances in late spring and summer (Figures S6a–S6c in the Supporting Information S1) are caused by high levels of vegetation during growing season (Burshtein et al., 2011) and photochemical reactions. However, only the biogenic emission factor had discernible contributions to $Abs_{365,w}$ in warm periods, which might be coming from water-soluble humic-like substances in resuspended soil (Trevisan et al., 2010; Wang, 2015).

The remaining two factors indicated secondary formations of $(NH_4)_2SO_4$ and NH_4NO_3, and contributed the largest portion of bulk components (~50%, Table S6 in the Supporting Information S1), which is in consistent with previous studies (Hua et al., 2015; Li et al., 2016; Yu et al., 2020). However, the presence of high MW PAHs and a *n*-alkane pattern of tire wear particles (Rogge et al., 1993b) suggested some influences from primary emissions. The average contributions of the secondary nitrate factor to $Abs_{365,w}$ and $Abs_{365,m}$ were $0.52 \pm 0.47\ Mm^{-1}$ and $0.54 \pm 0.50\ Mm^{-1}$, respectively, indicating that the light-absorbing OC apportioned to this factor was mostly water soluble. Several studies observed the formation of BrC from photo-oxidation of anthropogenic volatile organic compounds (VOCs, e.g., toluene) in the presence of NO_X (Lin, Liu, et al., 2015; Liu et al., 2016; Nakayama et al., 2010; Xie, Chen, et al., 2017). During that process, nitrophenol-like compounds (e.g., nitrocatechol, methyl nitrocatechols) can be generated (Iinuma et al., 2010), and they are water-soluble light-absorbing chromophores (Lin, Liu, et al., 2015; Xie, Chen, et al., 2017; Zhang et al., 2013). Moreover, certain types of SOA may become light-absorbing after reacting with reduced nitrogen compounds (e.g., NH_3, NH_4^+) (Lin, Laskin, et al., 2015; Updyke et al., 2012). It was also inferred form laboratory studies that oligomers containing nitroxy organosulphate groups formed in acidic aerosols are light-absorbing chromophores (Lin et al., 2014; Song et al., 2013). Due to the lack of appropriate OMMs, the formations of light-absorbing OC through gas-phase, aqueous, and/or heterogenous reactions might be lumped into the secondary nitrate factor, and more work is needed to quantify their contributions to BrC absorption.

4. Implications and Conclusions

In this work, collocated filter samples of ambient $PM_{2.5}$ obtained in northern Nanjing were analyzed for solvent extracts absorption, and a backup filter was used to address positive sampling artifacts. The collocated precision, parameterized using *r*, COD, and ARPD values, of light-absorbing properties of WSOC and MEOC prior to and after Q_b corrections indicated good agreement between collocated measurements. The light absorption of WSOC and MEOC will be significantly ($p < 0.05$) overestimated if positive sampling artifacts due to gaseous adsorption to filter medium are ignored. Due to the difference in Q_b corrections, the artifact-corrected data exhibited less similarity between collocated samples and had larger uncertainty than Q_f measurements. The estimated uncertainty of MEOC absorption (20%–30%) was much greater than that of WSOC absorption (10%–20%), suggesting that assuming a uniform uncertainty fraction (e.g., ~10%) for the light absorption of both water and methanol

extracts is not appropriate. Here, the uncertainty fractions of solvent extracts absorption based on duplicate artifact-corrected data could be used in future studies on BrC radiative forcing and source apportionment.

Nine specific source-related factors were identified by incorporating fifty OMMs with varying polarity for PMF analysis. Biomass burning activities are still the most important source of BrC absorption in winter periods. The meteorological conditions and transport of residential heating emissions are responsible for increased $Abs_{365,m}$ contributions of the coal combustion factor in winter. While the lubricating oil combustion factor showed elevated $Abs_{365,m}$ contributions in summer, probably due to decreased air density. As the dust associated organic matter experienced more heterogeneous aging than that from primary combustions, the dust resuspension factor had the second highest average contribution to $Abs_{365,w}$ (26.9%). The fractions of $Abs_{365,w}$ and $Abs_{365,m}$ loaded on the secondary nitrate factor might indicate the formation of light-absorbing OC though a variety of reactions with nitrogen containing species (e.g., NH_3, NO_X). Other factors, including non-combustion fossil, biogenic emission, isoprene oxidation, and secondary sulfate, were less related to $Abs_{365,w}$ and $Abs_{365,m}$, but their contributions to bulk $PM_{2.5}$ can never be neglected.

Conflict of Interest

The authors declare no conflicts of interest relevant to this study.

Data Availability Statement

Data used in the writing of this paper (and its in the Supporting Information S1) are publicly available on Harvard Dataverse (https://doi.org/10.7910/DVN/DBQIUJ).

Acknowledgments
This work was supported by the National Natural Science Foundation of China (NSFC, 42177211, 41701551). The authors declare that they have no conflict of interest.

References

Andreae, M. O., & Gelencsér, A. (2006). Black carbon or brown carbon? The nature of light-absorbing carbonaceous aerosols. *Atmospheric Chemistry and Physics*, *6*(10), 3131–3148. https://doi.org/10.5194/acp-6-3131-2006

Bond, T. C., & Bergstrom, R. W. (2006). Light absorption by carbonaceous particles: An investigative review. *Aerosol Science and Technology*, *40*(1), 27–67. https://doi.org/10.1080/02786820500421521

Burshtein, N., Lang-Yona, N., & Rudich, Y. (2011). Ergosterol, arabitol and mannitol as tracers for biogenic aerosols in the eastern Mediterranean. *Atmospheric Chemistry and Physics*, *11*(2), 829–839. https://doi.org/10.5194/acp-11-829-2011

Caravaggio, G. A., Charland, J.-P., Macdonald, P., & Graham, L. (2007). n-Alkane profiles of engine lubricating oil and particulate matter by molecular sieve extraction. *Environmental Science and Technology*, *41*(10), 3697–3701. https://doi.org/10.1021/es062233h

Chen, L. W. A., Doddridge, B. G., Dickerson, R. R., Chow, J. C., Mueller, P. K., Quinn, J., & Butler, W. A. (2001). Seasonal variations in elemental carbon aerosol, carbon monoxide and sulfur dioxide: Implications for sources. *Geophysical Research Letters*, *28*(9), 1711–1714. https://doi.org/10.1029/2000GL012354

Chen, Y., & Bond, T. C. (2010). Light absorption by organic carbon from wood combustion. *Atmospheric Chemistry and Physics*, *10*(4), 1773–1787. https://doi.org/10.5194/acp-10-1773-2010

Chow, J. C., Watson, J. G., Chen, L. W. A., Rice, J., & Frank, N. H. (2010). Quantification of PM2.5 organic carbon sampling artifacts in US networks. *Atmospheric Chemistry and Physics*, *10*(12), 5223–5239. https://doi.org/10.5194/acp-10-5223-2010

Claeys, M., Graham, B., Vas, G., Wang, W., Vermeylen, R., Pashynska, V., et al. (2004). Formation of secondary organic aerosols through photooxidation of isoprene. *Science*, *303*(5661), 1173–1176. https://doi.org/10.1126/science.1092805

Di Lorenzo, R. A., Washenfelder, R. A., Attwood, A. R., Guo, H., Xu, L., Ng, N. L., et al. (2017). Molecular-size-separated brown carbon absorption for biomass-burning aerosol at multiple field sites. *Environmental Science and Technology*, *51*(6), 3128–3137. https://doi.org/10.1021/acs.est.6b06160

Di Lorenzo, R. A., & Young, C. J. (2016). Size separation method for absorption characterization in brown carbon: Application to an aged biomass burning sample. *Geophysical Research Letters*, *43*(1), 458–465. https://doi.org/10.1002/2015GL066954

Dutton, S. J., Schauer, J. J., Vedal, S., & Hannigan, M. P. (2009). PM2.5 characterization for time series studies: Pointwise uncertainty estimation and bulk speciation methods applied in Denver. *Atmospheric Environment*, *43*(5), 1136–1146. https://doi.org/10.1016/j.atmosenv.2008.10.003

Feng, Y., Ramanathan, V., & Kotamarthi, V. R. (2013). Brown carbon: A significant atmospheric absorber of solar radiation? *Atmospheric Chemistry and Physics*, *13*(17), 8607–8621. https://doi.org/10.5194/acp-13-8607-2013

Flanagan, J. B., Jayanty, R. K. M., Rickman, J. E. E., & Peterson, M. R. (2006). PM2.5 speciation trends network: Evaluation of whole-system uncertainties using data from sites with collocated samplers. *Journal of the Air & Waste Management Association*, *56*(4), 492–499. https://doi.org/10.1080/10473289.2006.10464516

Gou, Y., Qin, C., Liao, H., & Xie, M. (2021). Measurements, gas/particle partitioning, and sources of nonpolar organic molecular markers at a suburban site in the west Yangtze River Delta, China. *Journal of Geophysical Research: Atmospheres*, *126*(19), e2020JD034080. https://doi.org/10.1029/2020JD034080

Hecobian, A., Zhang, X., Zheng, M., Frank, N., Edgerton, E. S., & Weber, R. J. (2010). Water-soluble organic aerosol material and the light-absorption characteristics of aqueous extracts measured over the Southeastern United States. *Atmospheric Chemistry and Physics*, *10*(13), 5965–5977. https://doi.org/10.5194/acp-10-5965-2010

Helin, A., Virkkula, A., Backman, J., Pirjola, L., Sippula, O., Aakko-Saksa, P., et al. (2021). Variation of absorption Ångström exponent in aerosols from different emission sources. *Journal of Geophysical Research: Atmospheres*, *126*(10), e2020JD034094. https://doi.org/10.1029/2020JD034094

Hua, Y., Cheng, Z., Wang, S., Jiang, J., Chen, D., Cai, S., et al. (2015). Characteristics and source apportionment of PM2.5 during a fall heavy haze episode in the Yangtze River Delta of China. *Atmospheric Environment*, *123*, 380–391. https://doi.org/10.1016/j.atmosenv.2015.03.046

Huang, R.-J., Yang, L., Cao, J., Chen, Y., Chen, Q., Li, Y., et al. (2018). Brown carbon aerosol in urban Xi'an, northwest China: The composition and light absorption properties. *Environmental Science and Technology*, *52*(12), 6825–6833. https://doi.org/10.1021/acs.est.8b02386

Huang, R.-J., Yang, L., Shen, J., Yuan, W., Gong, Y., Guo, J., et al. (2020). Water-insoluble organics dominate brown carbon in wintertime urban aerosol of China: Chemical characteristics and optical properties. *Environmental Science and Technology*, *54*(13), 7836–7847. https://doi.org/10.1021/acs.est.0c01149

Huang, R.-J., Zhang, Y., Bozzetti, C., Ho, K.-F., Cao, J.-J., Han, Y., et al. (2014). High secondary aerosol contribution to particulate pollution during haze events in China. *Nature*, *514*(7521), 218–222. https://doi.org/10.1038/nature13774

Human, D. M., Ullman, T. L., & Baines, T. M. (1990). Simulation of high altitude effects on heavy-duty diesel emissions. *SAE Transactions*, *99*, 1791–1800. https://doi.org/10.4271/900883

Hyslop, N. P., & White, W. H. (2008). An evaluation of interagency monitoring of protected visual environments (IMPROVE) collocated precision and uncertainty estimates. *Atmospheric Environment*, *42*(11), 2691–2705. https://doi.org/10.1016/j.atmosenv.2007.06.053

Iinuma, Y., Böge, O., Gräfe, R., & Herrmann, H. (2010). Methyl-nitrocatechols: Atmospheric tracer compounds for biomass burning secondary organic aerosols. *Environmental Science and Technology*, *44*(22), 8453–8459. https://doi.org/10.1021/es102938a

Jimenez, J. L., Canagaratna, M. R., Donahue, N. M., Prevot, A. S. H., Zhang, Q., Kroll, J. H., et al. (2009). Evolution of organic aerosols in the atmosphere. *Science*, *326*(5959), 1525–1529. https://doi.org/10.1126/science.1180353

Kim, E., & Hopke, P. K. (2007). Comparison between sample-species specific uncertainties and estimated uncertainties for the source apportionment of the speciation trends network data. *Atmospheric Environment*, *41*(3), 567–575. https://doi.org/10.1016/j.atmosenv.2006.08.023

Kim, E., Hopke, P. K., Pinto, J. P., & Wilson, W. E. (2005). Spatial variability of fine particle mass, components, and source contributions during the regional air pollution study in St. Louis. *Environmental Science and Technology*, *39*(11), 4172–4179. https://doi.org/10.1021/es049824x

Kirchstetter, T. W., Corrigan, C. E., & Novakov, T. (2001). Laboratory and field investigation of the adsorption of gaseous organic compounds onto quartz filters. *Atmospheric Environment*, *35*(9), 1663–1671. https://doi.org/10.1016/S1352-2310(00)00448-9

Kirchstetter, T. W., Novakov, T., & Hobbs, P. V. (2004). Evidence that the spectral dependence of light absorption by aerosols is affected by organic carbon. *Journal of Geophysical Research-Atmospheres*, *109*(D21), D21208. https://doi.org/10.1029/2004jd004999

Krudysz, M. A., Froines, J. R., Fine, P. M., & Sioutas, C. (2008). Intra-community spatial variation of size-fractionated PM mass, OC, EC, and trace elements in the Long Beach, CA area. *Atmospheric Environment*, *42*(21), 5374–5389. https://doi.org/10.1016/j.atmosenv.2008.02.060

Lack, D. A., Langridge, J. M., Bahreini, R., Cappa, C. D., Middlebrook, A. M., & Schwarz, J. P. (2012). Brown carbon and internal mixing in biomass burning particles. *Proceedings of the National Academy of Sciences of the United States of America*, *109*(37), 14802–14807. https://doi.org/10.1073/pnas.1206575109

Li, H., Wang, Q. G., Yang, M., Li, F., Wang, J., Sun, Y., et al. (2016). Chemical characterization and source apportionment of PM2.5 aerosols in a megacity of Southeast China. *Atmospheric Research*, *181*, 288–299. https://doi.org/10.1016/j.atmosres.2016.07.005

Li, X., Chen, Y., & Bond, T. C. (2016). Light absorption of organic aerosol from pyrolysis of corn stalk. *Atmospheric Environment*, *144*, 249–256. https://doi.org/10.1016/j.atmosenv.2016.09.006

Li, Y., Fu, T.-M., Yu, J. Z., Feng, X., Zhang, L., Chen, J., et al. (2021). Impacts of chemical degradation on the global budget of atmospheric levoglucosan and its use as a biomass burning tracer. *Environmental Science and Technology*, *55*(8), 5525–5536. https://doi.org/10.1021/acs.est.0c07313

Lin, P., Bluvshtein, N., Rudich, Y., Nizkorodov, S. A., Laskin, J., & Laskin, A. (2017). Molecular chemistry of atmospheric brown carbon inferred from a nationwide biomass burning event. *Environmental Science and Technology*, *51*(20), 11561–11570. https://doi.org/10.1021/acs.est.7b02276

Lin, P., Laskin, J., Nizkorodov, S. A., & Laskin, A. (2015). Revealing brown carbon chromophores produced in reactions of methylglyoxal with ammonium sulfate. *Environmental Science and Technology*, *49*(24), 14257–14266. https://doi.org/10.1021/acs.est.5b03608

Lin, P., Liu, J. M., Shilling, J. E., Kathmann, S. M., Laskin, J., & Laskin, A. (2015). Molecular characterization of brown carbon (BrC) chromophores in secondary organic aerosol generated from photo-oxidation of toluene. *Physical Chemistry Chemical Physics*, *17*(36), 23312–23325. https://doi.org/10.1039/c5cp02563j

Lin, Y.-H., Budisulistiorini, S. H., Chu, K., Siejack, R. A., Zhang, H., Riva, M., et al. (2014). Light-absorbing oligomer formation in secondary organic aerosol from reactive uptake of isoprene epoxydiols. *Environmental Science and Technology*, *48*(20), 12012–12021. https://doi.org/10.1021/es503142b

Liu, D., Lin, T., Syed, J. H., Cheng, Z., Xu, Y., Li, K., et al. (2017). Concentration, source identification, and exposure risk assessment of PM2.5-bound parent PAHs and nitro-PAHs in atmosphere from typical Chinese cities. *Scientific Reports*, *7*(1), 10398. https://doi.org/10.1038/s41598-017-10623-4

Liu, J., Bergin, M., Guo, H., King, L., Kotra, N., Edgerton, E., & Weber, R. J. (2013). Size-resolved measurements of brown carbon in water and methanol extracts and estimates of their contribution to ambient fine-particle light absorption. *Atmospheric Chemistry and Physics*, *13*(24), 12389–12404. https://doi.org/10.5194/acp-13-12389-2013

Liu, J., Lin, P., Laskin, A., Laskin, J., Kathmann, S. M., Wise, M., et al. (2016). Optical properties and aging of light-absorbing secondary organic aerosol. *Atmospheric Chemistry and Physics*, *16*(19), 12815–12827. https://doi.org/10.5194/acp-16-12815-2016

Liu, Y., Yan, C., Ding, X., Wang, X., Fu, Q., Zhao, Q., et al. (2017). Sources and spatial distribution of particulate polycyclic aromatic hydrocarbons in Shanghai, China. *The Science of the Total Environment*, *584–585*, 307–317. https://doi.org/10.1016/j.scitotenv.2016.12.134

Maria, S. F., Russell, L. M., Gilles, M. K., & Myneni, S. C. J. S. (2004). Organic aerosol growth mechanisms and their climate-forcing implications. *Science*, *306*(5703), 1921–1924. https://doi.org/10.1126/science.1103491

Nakayama, T., Matsumi, Y., Sato, K., Imamura, T., Yamazaki, A., & Uchiyama, A. (2010). Laboratory studies on optical properties of secondary organic aerosols generated during the photooxidation of toluene and the ozonolysis of α-pinene. *Journal of Geophysical Research: Atmospheres*, *115*(D24), D24204. https://doi.org/10.1029/2010jd014387

Paatero, P., & Hopke, P. K. (2003). Discarding or downweighting high-noise variables in factor analytic models. *Analytica Chimica Acta*, *490*(1–2), 277–289. https://doi.org/10.1016/S0003-2670(02)01643-4

Pokhrel, R. P., Beamesderfer, E. R., Wagner, N. L., Langridge, J. M., Lack, D. A., Jayarathne, T., et al. (2017). Relative importance of black carbon, brown carbon, and absorption enhancement from clear coatings in biomass burning emissions. *Atmospheric Chemistry and Physics*, *17*(8), 5063–5078. https://doi.org/10.5194/acp-17-5063-2017

Polissar, A. V., Hopke, P. K., & Paatero, P. (1998). Atmospheric aerosol over Alaska - 2. Elemental composition and sources. *Journal of Geophysical Research: Atmospheres*, *103*(D15), 19045–19057. https://doi.org/10.1029/98jd01212

Qin, C., Gou, Y., Wang, Y., Mao, Y., Liao, H., Wang, Q., & Xie, M. (2021). Gas–particle partitioning of polyol tracers at a suburban site in Nanjing, east China: Increased partitioning to the particle phase. *Atmospheric Chemistry and Physics*, *21*(15), 12141–12153. https://doi.org/10.5194/acp-21-12141-2021

Rogge, W. F., Hildemann, L. M., Mazurek, M. A., Cass, G. R., & Simoneit, B. R. T. (1993a). Sources of fine organic aerosol .2. Noncatalyst and catalyst-equipped automobiles and heavy-duty diesel trucks. *Environmental Science and Technology*, *27*(4), 636–651. https://doi.org/10.1021/es00041a007

Rogge, W. F., Hildemann, L. M., Mazurek, M. A., Cass, G. R., & Simoneit, B. R. T. (1993b). Sources of fine organic aerosol .3. Road dust, tire debris, and organometallic brake lining dust - Roads as sources and sinks. *Environmental Science and Technology*, *27*(9), 1892–1904. https://doi.org/10.1021/es00046a019

Rogge, W. F., Hildemann, L. M., Mazurek, M. A., Cass, G. R., & Simoneit, B. R. T. (1993c). Sources of fine organic aerosol .4. Particulate abrasion products from leaf surfaces of urban plants. *Environmental Science and Technology*, *27*(13), 2700–2711. https://doi.org/10.1021/es00049a008

Saleh, R., Hennigan, C. J., McMeeking, G. R., Chuang, W. K., Robinson, E. S., Coe, H., et al. (2013). Absorptivity of brown carbon in fresh and photo-chemically aged biomass-burning emissions. *Atmospheric Chemistry and Physics*, *13*(15), 7683–7693. https://doi.org/10.5194/acp-13-7683-2013

Saleh, R., Marks, M., Heo, J., Adams, P. J., Donahue, N. M., & Robinson, A. L. (2015). Contribution of brown carbon and lensing to the direct radiative effect of carbonaceous aerosols from biomass and biofuel burning emissions. *Journal of Geophysical Research: Atmospheres*, *120*(19), 10285–10296. https://doi.org/10.1002/2015JD023697

Saleh, R., Robinson, E. S., Tkacik, D. S., Ahern, A. T., Liu, S., Aiken, A. C., et al. (2014). Brownness of organics in aerosols from biomass burning linked to their black carbon content. *Nature Geoscience*, *7*(9), 647–650. https://doi.org/10.1038/ngeo2220

Samburova, V., Connolly, J., Gyawali, M., Yatavelli, R. L. N., Watts, A. C., Chakrabarty, R. K., et al. (2016). Polycyclic aromatic hydrocarbons in biomass-burning emissions and their contribution to light absorption and aerosol toxicity. *The Science of the Total Environment*, *568*, 391–401. https://doi.org/10.1016/j.scitotenv.2016.06.026

Schauer, J. J., Kleeman, M. J., Cass, G. R., & Simoneit, B. R. T. (1999). Measurement of emissions from air pollution sources. 2. C-1 through C-30 organic compounds from medium duty diesel trucks. *Environmental Science and Technology*, *33*(10), 1578–1587. https://doi.org/10.1021/es980081n

Schauer, J. J., Kleeman, M. J., Cass, G. R., & Simoneit, B. R. T. (2002). Measurement of emissions from air pollution sources. 5. C-1-C-32 organic compounds from gasoline-powered motor vehicles. *Environmental Science and Technology*, *36*(6), 1169–1180. https://doi.org/10.1021/es0108077

Sillanpää, M., Frey, A., Hillamo, R., Pennanen, A. S., & Salonen, R. O. (2005). Organic, elemental and inorganic carbon in particulate matter of six urban environments in Europe. *Atmospheric Chemistry and Physics*, *5*(11), 2869–2879. https://doi.org/10.5194/acp-5-2869-2005

Simoneit, B. R. T., Elias, V. O., Kobayashi, M., Kawamura, K., Rushdi, A. I., Medeiros, P. M., et al. (2004). Sugars – Dominant water-soluble organic compounds in soils and characterization as tracers in atmospheric particulate matter. *Environmental Science and Technology*, *38*(22), 5939–5949. https://doi.org/10.1021/es0403099

Simoneit, B. R. T., Schauer, J. J., Nolte, C. G., Oros, D. R., Elias, V. O., Fraser, M. P., et al. (1999). Levoglucosan, a tracer for cellulose in biomass burning and atmospheric particles. *Atmospheric Environment*, *33*(2), 173–182. https://doi.org/10.1016/S1352-2310(98)00145-9

Song, C., Gyawali, M., Zaveri, R. A., Shilling, J. E., & Arnott, W. P. (2013). Light absorption by secondary organic aerosol from α-pinene: Effects of oxidants, seed aerosol acidity, and relative humidity. *Journal of Geophysical Research: Atmospheres*, *118*(2011), 741749–711. https://doi.org/10.1002/jgrd.50767

Subramanian, R., Khlystov, A. Y., Cabada, J. C., & Robinson, A. L. (2004). Positive and negative artifacts in particulate organic carbon measurements with denuded and undenuded sampler configurations special issue of aerosol science and technology on findings from the fine particulate matter supersites program. *Aerosol Science and Technology*, *38*(sup1), 27–48. https://doi.org/10.1080/02786820390229354

Surratt, J. D., Murphy, S. M., Kroll, J. H., Ng, N. L., Hildebrandt, L., Sorooshian, A., et al. (2006). Chemical composition of secondary organic aerosol formed from the photooxidation of isoprene. *The Journal of Physical Chemistry A*, *110*(31), 9665–9690. https://doi.org/10.1021/jp061734m

Trevisan, S., Francioso, O., Quaggiotti, S., & Nardi, S. (2010). Humic substances biological activity at the plant-soil interface. *Plant Signaling & Behavior*, *5*(6), 635–643. https://doi.org/10.4161/psb.5.6.11211

Updyke, K. M., Nguyen, T. B., & Nizkorodov, S. A. (2012). Formation of brown carbon via reactions of ammonia with secondary organic aerosols from biogenic and anthropogenic precursors. *Atmospheric Environment*, *63*, 22–31. https://doi.org/10.1016/j.atmosenv.2012.09.012

Wang, N. (2015). *Size distribution characteristics of ambient aerosol in urban Hong Kong: Major chemical components and light extinction estimation*. Hong Kong University of Science and Technology. Thesis (M.Phil.). https://doi.org/10.14711/thesis-b1514662

Wang, Q., Ye, J., Wang, Y., Zhang, T., Ran, W., Wu, Y., et al. (2019). Wintertime optical properties of primary and secondary brown carbon at a regional site in the north China plain. *Environmental Science and Technology*, *53*(21), 12389–12397. https://doi.org/10.1021/acs.est.9b03406

Wang, X., Heald, C. L., Ridley, D. A., Schwarz, J. P., Spackman, J. R., Perring, A. E., et al. (2014). Exploiting simultaneous observational constraints on mass and absorption to estimate the global direct radiative forcing of black carbon and brown carbon. *Atmospheric Chemistry and Physics*, *14*(20), 10989–11010. https://doi.org/10.5194/acp-14-10989-2014

Wang, Y., Zhang, Q., Zhang, Y., Zhao, H., Tan, F., Wu, X., & Chen, J. (2019). Source apportionment of polycyclic aromatic hydrocarbons (PAHs) in the air of Dalian, China: Correlations with six criteria air pollutants and meteorological conditions. *Chemosphere*, *216*, 516–523. https://doi.org/10.1016/j.chemosphere.2018.10.184

Wilson, J. G., Kingham, S., Pearce, J., & Sturman, A. P. (2005). A review of intraurban variations in particulate air pollution: Implications for epidemiological research. *Atmospheric Environment*, *39*(34), 6444–6462. https://doi.org/10.1016/j.atmosenv.2005.07.030

Wongphatarakul, V., Friedlander, S. K., & Pinto, J. P. (1998). A comparative study of PM2.5 ambient aerosol chemical databases. *Environmental Science and Technology*, *32*(24), 3926–3934. https://doi.org/10.1021/es9800582

Xie, M., Barsanti, K. C., Hannigan, M. P., Dutton, S. J., & Vedal, S. (2013). Positive matrix factorization of PM2.5 - Eliminating the effects of gas/particle partitioning of semivolatile organic compounds. *Atmospheric Chemistry and Physics*, *13*(15), 7381–7393. https://doi.org/10.5194/acp-13-7381-2013

Xie, M., Chen, X., Hays, M. D., & Holder, A. L. (2019). Composition and light absorption of N-containing aromatic compounds in organic aerosols from laboratory biomass burning. *Atmospheric Chemistry and Physics*, *19*(5), 2899–2915. https://doi.org/10.5194/acp-19-2899-2019

Xie, M., Chen, X., Hays, M. D., Lewandowski, M., Offenberg, J., Kleindienst, T. E., & Holder, A. L. (2017). Light absorption of secondary organic aerosol: Composition and contribution of nitroaromatic compounds. *Environmental Science and Technology*, *51*(20), 11607–11616. https://doi.org/10.1021/acs.est.7b03263

Xie, M., Chen, X., Holder, A. L., Hays, M. D., Lewandowski, M., Offenberg, J. H., et al. (2019). Light absorption of organic carbon and its sources at a southeastern U.S. location in summer. *Environmental Pollution*, *244*, 38–46. https://doi.org/10.1016/j.envpol.2018.09.125

Xie, M., Coons, T. L., Dutton, S. J., Milford, J. B., Miller, S. L., Peel, J. L., et al. (2012). Intra-urban spatial variability of PM2.5-bound carbonaceous components. *Atmospheric Environment*, *60*(0), 486–494. https://doi.org/10.1016/j.atmosenv.2012.05.041

Xie, M., Hannigan, M. P., & Barsanti, K. C. (2014). Impact of gas/particle partitioning of semivolatile organic compounds on source apportionment with positive matrix factorization. *Environmental Science and Technology*, *48*(16), 9053–9060. https://doi.org/10.1021/es5022262

Xie, M., Hays, M. D., & Holder, A. L. (2017). Light-absorbing organic carbon from prescribed and laboratory biomass burning and gasoline vehicle emissions. *Scientific Reports*, *7*(1), 7318. https://doi.org/10.1038/s41598-017-06981-8

Xie, M., Mladenov, N., Williams, M. W., Neff, J. C., Wasswa, J., & Hannigan, M. P. (2016). Water soluble organic aerosols in the Colorado rocky Mountains, USA: Composition, sources and optical properties. *Scientific Reports*, *6*, 39339. https://doi.org/10.1038/srep39339

Xie, M., Piedrahita, R., Dutton, S. J., Milford, J. B., Hemann, J. G., Peel, J. L., et al. (2013). Positive matrix factorization of a 32-month series of daily PM2.5 speciation data with incorporation of temperature stratification. *Atmospheric Environment*, *65*(0), 11–20. https://doi.org/10.1016/j.atmosenv.2012.09.034

Xie, M., Shen, G., Holder, A. L., Hays, M. D., & Jetter, J. J. (2018). Light absorption of organic carbon emitted from burning wood, charcoal, and kerosene in household cookstoves. *Environmental Pollution*, *240*, 60–67. https://doi.org/10.1016/j.envpol.2018.04.085

Xie, M., Zhao, Z., Holder, A. L., Hays, M. D., Chen, X., Shen, G., et al. (2020). Chemical composition, structures, and light absorption of N-containing aromatic compounds emitted from burning wood and charcoal in household cookstoves. *Atmospheric Chemistry and Physics*, *20*(22), 14077–14090. https://doi.org/10.5194/acp-20-14077-2020

Yan, D., Wu, S., Zhou, S., Tong, G., Li, F., Wang, Y., & Li, B. (2019). Characteristics, sources and health risk assessment of airborne particulate PAHs in Chinese cities: A review. *Environmental Pollution*, *248*, 804–814. https://doi.org/10.1016/j.envpol.2019.02.068

Yang, L., Shang, Y., Hannigan, M. P., Zhu, R., Wang, Q. G., Qin, C., & Xie, M. (2021). Collocated speciation of PM2.5 using tandem quartz filters in northern Nanjing, China: Sampling artifacts and measurement uncertainty. *Atmospheric Environment*, *246*, 118066. https://doi.org/10.1016/j.atmosenv.2020.118066

Yang, M., Howell, S. G., Zhuang, J., & Huebert, B. J. (2009). Attribution of aerosol light absorption to black carbon, brown carbon, and dust in China – Interpretations of atmospheric measurements during EAST-AIRE. *Atmospheric Chemistry and Physics*, *9*(6), 2035–2050. https://doi.org/10.5194/acp-9-2035-2009

Yu, Y., Ding, F., Mu, Y., Xie, M., & Wang, Q. g. (2020). High time-resolved PM2.5 composition and sources at an urban site in Yangtze River Delta, China after the implementation of the APPCAP. *Chemosphere*, *261*, 127746. https://doi.org/10.1016/j.chemosphere.2020.127746

Yu, Y., He, S., Wu, X., Zhang, C., Yao, Y., Liao, H., et al. (2019). PM2.5 elements at an urban site in Yangtze River Delta, China: High time-resolved measurement and the application in source apportionment. *Environmental Pollution*, *253*, 1089–1099. https://doi.org/10.1016/j.envpol.2019.07.096

Zhang, X., Lin, Y.-H., Surratt, J. D., & Weber, R. J. (2013). Sources, composition and absorption Ångström exponent of light-absorbing organic components in aerosol extracts from the Los Angeles basin. *Environmental Science and Technology*, *47*(8), 3685–3693. https://doi.org/10.1021/es305047b

Zhang, X., Lin, Y.-H., Surratt, J. D., Zotter, P., Prévôt, A. S. H., & Weber, R. J. (2011). Light-absorbing soluble organic aerosol in Los Angeles and Atlanta: A contrast in secondary organic aerosol. *Geophysical Research Letters*, *38*(21), L21810. https://doi.org/10.1029/2011GL049385

Zhang, Y., Forrister, H., Liu, J., Dibb, J., Anderson, B., Schwarz, J. P., et al. (2017). Top-of-atmosphere radiative forcing affected by brown carbon in the upper troposphere. *Nature Geoscience*, *10*(7), 486. https://doi.org/10.1038/ngeo2960

Zhu, C.-S., Li, L.-J., Huang, H., Dai, W.-T., Lei, Y.-L., Qu, Y., et al. (2020). n-Alkanes and PAHs in the southeastern Tibetan plateau: Characteristics and correlations with brown carbon light absorption. *Journal of Geophysical Research: Atmospheres*, *125*(19), e2020JD032666. https://doi.org/10.1029/2020JD032666

References From the Supporting Information

Brown, S. G., Eberly, S., Paatero, P., & Norris, G. A. (2015). Methods for estimating uncertainty in PMF solutions: Examples with ambient air and water quality data and guidance on reporting PMF results. *The Science of the Total Environment*, *518–519*, 626–635. https://doi.org/10.1016/j.scitotenv.2015.01.022

Chen, D., Zhao, Y., Lyu, R., Wu, R., Dai, L., Zhao, Y., et al. (2019). Seasonal and spatial variations of optical properties of light absorbing carbon and its influencing factors in a typical polluted city in Yangtze River Delta, China. *Atmospheric Environment*, *199*, 45–54. https://doi.org/10.1016/j.atmosenv.2018.11.022

Chen, Y., Xie, X., Shi, Z., Li, Y., Gai, X., Wang, J., et al. (2020). Brown carbon in atmospheric fine particles in Yangzhou, China: Light absorption properties and source apportionment. *Atmospheric Research*, *244*, 105028. https://doi.org/10.1016/j.atmosres.2020.105028

Cheng, Y., He, K.-b., Du, Z.-y., Engling, G., Liu, J.-m., Ma, Y.-l., et al. (2016). The characteristics of brown carbon aerosol during winter in Beijing. *Atmospheric Environment*, *127*, 355–364. https://doi.org/10.1016/j.atmosenv.2015.12.035

Liu, B., Wu, J., Zhang, J., Wang, L., Yang, J., Liang, D., et al. (2017). Characterization and source apportionment of PM2.5 based on error estimation from EPA PMF 5.0 model at a medium city in China. *Environmental Pollution*, *222*, 10–22. https://doi.org/10.1016/j.envpol.2017.01.005

Norris, G., Duvall, R., Brown, S., & Bai, S. (2014). *EPA positive matrix factorization (PMF) 5.0 fundamentals and user guide prepared for the*. US Environmental Protection Agency office of research and development. Retrieved from https://www.epa.gov/air-research/epa-positive-matrix-factorization-50-fundamentals-and-user-guide

Paatero, P., Eberly, S., Brown, S. G., & Norris, G. A. (2014). Methods for estimating uncertainty in factor analytic solutions. *Atmospheric Measurement Techniques*, *7*(3), 781–797. https://doi.org/10.5194/amt-7-781-2014

Xie, M., Barsanti, K. C., Hannigan, M. P., Dutton, S. J., & Vedal, S. (2013). Positive matrix factorization of PM2.5 - Eliminating the effects of gas/particle partitioning of semivolatile organic compounds. *Atmospheric Chemistry and Physics*, *13*(15), 7381–7393. https://doi.org/10.5194/acp-13-7381-2013

Xie, M., Chen, X., Holder, A. L., Hays, M. D., Lewandowski, M., Offenberg, J. H., et al. (2019). Light absorption of organic carbon and its sources at a southeastern U.S. location in summer. *Environmental Pollution*, *244*, 38–46. https://doi.org/10.1016/j.envpol.2018.09.125

Xie, X., Chen, Y., Nie, D., Liu, Y., Liu, Y., Lei, R., et al. (2020). Light-absorbing and fluorescent properties of atmospheric brown carbon: A case study in Nanjing, China. *Chemosphere*, *251*, 126350. https://doi.org/10.1016/j.chemosphere.2020.126350

Yuan, W., Huang, R. J., Yang, L., Guo, J., Chen, Z., Duan, J., et al. (2020). Characterization of the light-absorbing properties, chromophore composition and sources of brown carbon aerosol in Xi'an, northwestern China. *Atmospheric Chemistry and Physics*, *20*(8), 5129–5144. https://doi.org/10.5194/acp-20-5129-2020